

## Effect of dislocation density on efficiency droop in GaInN/GaN light-emitting diodes

Martin F. Schubert, Sameer Chhajed, Jong Kyu Kim, and E. Fred Schubert<sup>a)</sup>

*Future Chips Constellation, Department of Electrical, Computer, and Systems Engineering, Rensselaer Polytechnic Institute, Troy, New York 12180, USA*

Daniel D. Koleske, Mary H. Crawford, Stephen R. Lee, Arthur J. Fischer, Gerald Thaler, and Michael A. Banas

*Sandia National Laboratories, Albuquerque, New Mexico 87185, USA*

(Received 27 August 2007; accepted 16 November 2007; published online 7 December 2007)

Measurements of light-output power versus current are performed for GaInN/GaN light-emitting diodes grown on GaN-on-sapphire templates with different threading dislocation densities. Low-defect-density devices exhibit a pronounced efficiency peak followed by droop as current increases, whereas high-defect-density devices show low peak efficiencies and little droop. The experimental data are analyzed with a rate equation model to explain this effect. Analysis reveals that dislocations do not strongly impact high-current performance; instead they contribute to increased nonradiative recombination at lower currents and a suppression of peak efficiency. The characteristics of the dominant recombination mechanism at high currents are consistent with processes involving carrier leakage. © 2007 American Institute of Physics.

[DOI: [10.1063/1.2822442](https://doi.org/10.1063/1.2822442)]

The *efficiency droop*, prominent in GaInN-based light-emitting *pn*-junction devices, is the gradual decrease of the power efficiency as the injection current increases. This phenomenon is a severe problem for high-power light-emitting diodes (LEDs) which operate at inherently high current densities. Understanding and mitigating efficiency droop is especially critical to attaining viable LEDs for solid-state lighting applications.

The efficiency droop results from a nonradiative carrier loss mechanism that has little relevance at low forward currents but becomes larger as the current increases. Several explanations for efficiency droop have been proposed, including carrier leakage at high forward currents,<sup>1–3</sup> Auger recombination,<sup>4</sup> junction heating,<sup>5</sup> and carrier delocalization from In-rich low-defect-density regions at high carrier densities.<sup>6,7</sup> In addition, it has been shown that the reduced dislocation density attainable for growth on GaN bulk substrates (compared with sapphire substrates) can influence the magnitude efficiency droop.<sup>8</sup>

In this work, we seek to clarify the efficiency droop mechanism by analyzing the light output of GaInN LEDs with a rate equation model that allows us to determine the relative radiative and nonradiative recombination rates, as well as the additional carrier loss term that produces the droop at high currents. We examine the effect of dislocation density on efficiency droop through the evaluation of GaInN LEDs grown on GaN-on-sapphire templates with low and high threading dislocation densities, and compare the characteristics of the three recombination terms for LEDs on these two templates—with a particular focus on the droop-inducing carrier-loss mechanism. This approach enables us to characterize the competition between recombination mechanisms in GaInN LEDs as a function of forward current and dislocation density, providing direct insight into the na-

ture of the carrier loss mechanism that dominates in the high current regime.

The GaInN LEDs used in this study are grown on *c*-plane sapphire using metal-organic chemical vapor deposition in a Veeco D-125 reactor. Threading dislocation densities in the GaN templates used for LED growths are controlled by varying nucleation-layer-growth and film-coalescence parameters,<sup>9,10</sup> and are verified after growth using x-ray diffraction.<sup>11</sup> For consistency, LED structures are concurrently grown in a subsequent growth run using *n*-type GaN-on-sapphire templates with different dislocation densities. The LED heterostructure is characterized by x-ray diffraction and *in situ* optical reflectance,<sup>12</sup> and consists of five 2.4-nm-thick Ga<sub>0.87</sub>In<sub>0.13</sub>N quantum wells sandwiched between 7.5-nm-thick Si-doped GaN barriers followed by a 30-nm-thick *p*-type Al<sub>0.15</sub>Ga<sub>0.85</sub>N electron-block layer and a 400-nm-thick *p*-type GaN contact layer. The resulting active region emits at a wavelength of 440 nm. Devices are processed as mesa structures of 200 × 200 μm<sup>2</sup> areas through inductively coupled plasma etching. *N*-type contacts consist of a TiAlNiAu multilayer stack, and a semitransparent NiO/Au contact is applied to the *p* side of the device.

Two representative samples—samples A and B, with measured total threading dislocation densities of 5.3 × 10<sup>8</sup> and 5.7 × 10<sup>9</sup> cm<sup>-2</sup>—are investigated. Figure 1(a) compares the light-output power and forward voltage of the two samples as a function of current (pulsed mode); Fig. 1(b) shows the external quantum efficiency. Sample B exhibits little change in the efficiency as current increases, but has low peak efficiency. In contrast, sample A has a peak efficiency that is more than double that of sample B. The peak efficiency for sample A occurs at approximately 12 mA; however, as the forward current is increased to 100 mA, efficiency is reduced by 23%. Thus, the two types of devices behave in distinctly different ways; high-defect-density devices have low peak efficiency but little droop while low-defect-density devices have high peak efficiency at low currents but also exhibit a substantial efficiency droop.

<sup>a)</sup>Electronic mail: [efschubert@rpi.edu](mailto:efschubert@rpi.edu).

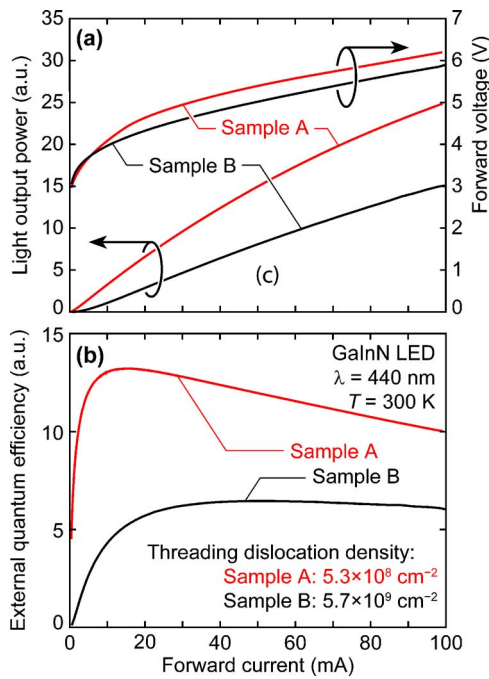


FIG. 1. (Color online) (a) Light-output power, forward voltage, and (b) efficiency as a function of current for the two samples.

The measured data are analyzed using a rate equation model in order to extract the rates of the various recombination mechanisms. In this model, the carrier density  $n$  is described by

$$\frac{dn}{dt} = \frac{I_f}{qV} - An - Bn^2 - f(n), \quad (1)$$

which is equal to zero at steady state. Here,  $I_f$  is the forward current,  $V$  is the active region volume, and  $A$  and  $B$  are the monomolecular nonradiative and bimolecular radiative recombination coefficients. We also include an additional carrier loss mechanism  $f$  which is important at high currents. Tentatively, this loss is attributed to decreased injection efficiency resulting in an electron leakage from the active region;<sup>1-3</sup> later we will show that this explanation is consistent with the results presented here. The three recombination mechanisms are illustrated in Fig. 2. The internal and external quantum efficiencies of a LED may be written in terms of these recombination mechanisms as

$$\text{EQE} = \eta_e \text{IQE} = \eta_e \frac{Bn^2}{An + Bn^2 + f(n)}, \quad (2)$$

where  $\eta_e$  is the light-extraction efficiency. Since the total number of photons generated is given by the product of the spontaneous emission rate  $Bn^2$  and the active region volume

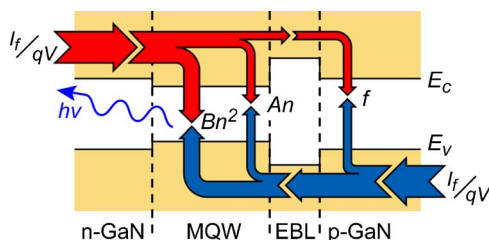


FIG. 2. (Color online) Schematic illustration of the three recombination mechanisms considered in this work.

$V$ , the measured photocurrent  $I_d$  is given by  $I_d = q\eta V B n^2$ , where the factor  $\eta$  depends upon the light-extraction efficiency, the fraction of emitted photons that are collected by the detector, and the quantum efficiency of the detector;  $\eta$  is taken to be equal for both samples. For the bimolecular recombination coefficient  $B$ , we have assumed a value of  $1 \times 10^{-10}$  cm $^3$  s $^{-1}$ , which is a typical number.<sup>13</sup> Once  $I_d$ ,  $\eta$ ,  $B$ , and  $V$  are known, the carrier density as a function of forward current can be found.

The monomolecular recombination rate can then be determined by fitting the light-output-versus-current curve at low forward current values, where  $f$  can be neglected. Using the extracted values for  $n$ , the curve in Fig. 1(a) is fitted by choosing the value for  $A$ . The form of the monomolecular recombination term  $An$  is valid under the conditions of equal high-level injection of electrons and holes. Because this condition is not exactly met in practice, and to allow for a closer fit to the measured data, the exponent of the carrier density in the monomolecular recombination term is allowed to deviate slightly from 1. For samples A and B this exponent is 1.2 and 0.76, respectively. The nonradiative recombination term can also be written in terms of a carrier-density-dependent lifetime,  $R_{nr} = n/\tau_{nr}(n)$ . At a density of  $10^{18}$  cm $^{-3}$ , the nonradiative lifetimes are 12.3 and 6.4 ns for samples A and B, respectively.

Figure 3(a) compares the measured external quantum efficiency with the efficiency calculated from Eq. (2) using the above estimates of the rate parameters  $A$  and  $B$ , and the leakage term set to zero ( $f=0$ ) as a function of current and carrier density. When the current remains below 5 mA, a good match is achieved with only the monomolecular recombination and spontaneous emission terms. At approximately 10 mA, the peak efficiency in sample A is reached and the droop begins. To obtain the additional carrier loss term  $f$  that causes the droop, we simply take the difference between the fitted and measured curves shown in Fig. 3(a).

Figure 3(b) shows the extracted rates for monomolecular recombination, spontaneous emission, and carrier leakage. In each of the two samples, nonradiative recombination is dominant at low currents. However, radiative recombination is more than ten times larger in sample A than in sample B. As the current increases, radiative recombination increases and eventually becomes larger than nonradiative recombination. This transition occurs at approximately 10 mA in sample A, and at 70 mA in Sample B. This is due to the shorter nonradiative lifetime for carriers resulting from the high dislocation density in Sample B.

In contrast to radiative and nonradiative recombinations, the carrier leakage  $f$  as a function of current is quantitatively very similar for the two devices. In both cases, the leakage term has the greatest slope; when the current increases, the fraction of carriers that are lost to leakage grows rapidly. At 100 mA, leakage constitutes 62.6% and 51.5% of total recombination for samples A and B, respectively. Given the very high threading dislocation density present in sample B compared to sample A, the close quantitative agreement of the leakage term in the two samples indicates the absence of a strong dependence of efficiency droop on dislocation density. In addition, since samples A and B have different radiative and nonradiative rates and carrier densities at a given injection current, the leakage term is not a direct function of carrier density and is not dependent on the radiative and nonradiative recombination mechanisms in the active region.

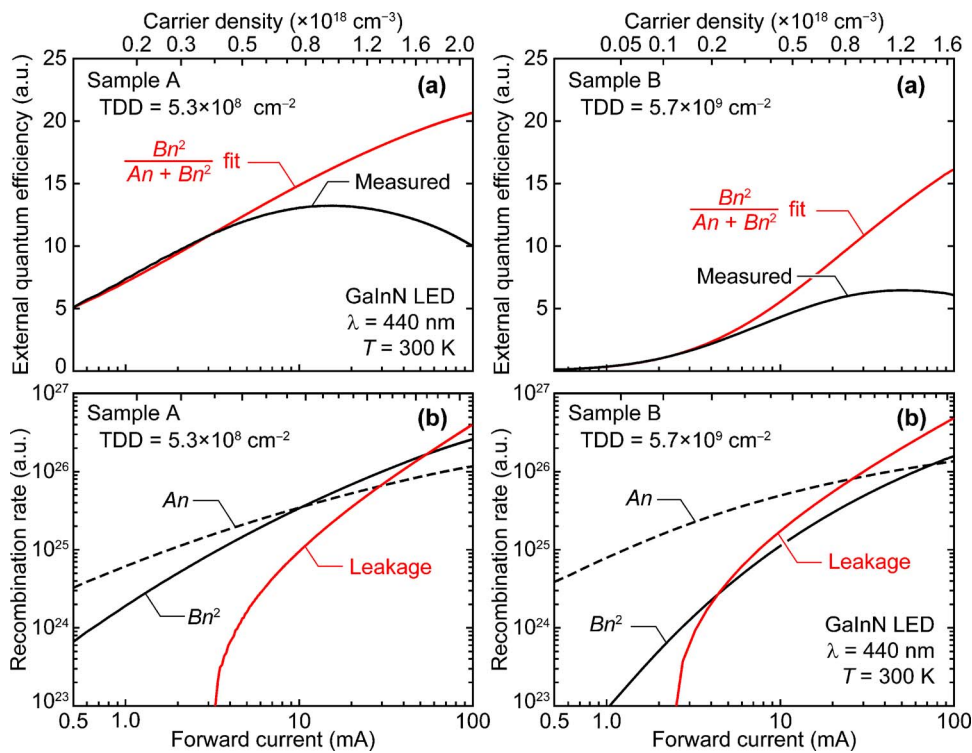


FIG. 3. (Color online) (a) Measured and fit external quantum efficiencies as well as (b) the three recombination mechanisms as a function of forward current.

Instead, the leakage term  $f$  depends primarily on the forward current. These characteristics are consistent with the carrier leakage explanation for the efficiency droop.

Taken together, the effect of dislocations on the nonradiative lifetime and the independence of leakage from the carrier density explain the presence of strong efficiency droop in sample A and its weakness in sample B. The onset of leakage at high currents means that peak efficiency is achieved at low currents. However, in sample B, the short nonradiative lifetime suppresses radiative recombination at low currents. Thus, while in sample A radiative recombination is the dominant mechanism from 10 to 30 mA, in sample B, radiative recombination is *never* dominant, and the efficiency remains low and lacks a pronounced peak.

In conclusion, we have performed experimental measurements of light-output power as a function of forward current for GaInN/GaN LEDs grown on GaN templates with different dislocation densities. Devices with low defect density have a high peak in efficiency, followed by the significant efficiency droop as the current increases. In contrast, high-defect-density samples have low peak efficiency, but also show little efficiency droop for large currents. A rate equation model is used to explain these trends in terms of the competition between monomolecular nonradiative recombination, radiative recombination, and an additional recombination term that dominates at high currents. Our analysis reveals that this high-current recombination term is quantitatively very similar for LEDs of different dislocation densities, thereby indicating that dislocations are not driving the efficiency droop at high currents. Instead, the primary effect of dislocations is in the low current regime where high defect densities correlate with increased dominance of nonradiative recombination and a pronounced suppression of the peak efficiency. The high-current recombination term is independent of dislocation density, as well as the monomolecular nonra-

diative and radiative recombination rates. This independence, along with the strikingly similar forward-current dependence for each sample, is consistent with a carrier leakage mechanism at high currents.

The authors from RPI acknowledge Sandia National Laboratories and the Department of Energy. Sandia is a multiprogram laboratory operated by Sandia Corporation, a Lockheed Martin Company, for the United States Department of Energy's National Nuclear Security Administration under Contract No. DE-AC04-94AL85000.

- <sup>1</sup>I. V. Rozhansky and D. A. Zakheim, *Phys. Status Solidi C* **3**, 2160 (2006).
- <sup>2</sup>I. V. Rozhansky and D. A. Zakheim, *Phys. Status Solidi A* **204**, 227 (2007).
- <sup>3</sup>M. H. Kim, M. F. Schubert, Q. Dai, J. K. Kim, E. F. Schubert, J. Piprek, and Y. Park, *Appl. Phys. Lett.* **91**, 183507 (2007).
- <sup>4</sup>Y. C. Shen, G. O. Mueller, S. Watanabe, N. F. Gardner, A. Munkholm, and M. R. Krames, *Appl. Phys. Lett.* **91**, 141101 (2007).
- <sup>5</sup>A. A. Efremov, N. I. Bochkareva, R. I. Gorbunov, D. A. Larinovich, Yu. T. Rebane, D. V. Tarkhin, and Yu. G. Shreter, *Semiconductors* **40**, 605 (2006).
- <sup>6</sup>A. Y. Kim, W. Götz, D. A. Steigerwald, J. J. Wierer, N. F. Gardner, J. Sun, S. A. Stockman, P. S. Martin, M. R. Krames, R. S. Kern, and F. M. Steranka, *Phys. Status Solidi A* **188**, 15 (2001).
- <sup>7</sup>S. F. Chichibu, T. Azuhata, M. Sugiyama, T. Kitamura, Y. Ishida, H. Okumura, H. Nakanishi, T. Sota, and T. Mukai, *J. Vac. Sci. Technol. B* **19**, 2177 (2001).
- <sup>8</sup>K. Akita, T. Kyono, Y. Yoshizumi, H. Kitabayashi, and K. Katayama, *J. Appl. Phys.* **101**, 033104 (2007).
- <sup>9</sup>D. D. Koleske, A. J. Fischer, A. A. Allerman, C. C. Mitchell, K. C. Cross, S. R. Kurtz, J. J. Figiel, K. W. Fullmer, and W. G. Breiland, *Appl. Phys. Lett.* **81**, 1940 (2002).
- <sup>10</sup>D. D. Koleske and S. R. Lee (unpublished).
- <sup>11</sup>S. R. Lee, A. M. West, A. A. Allerman, K. E. Waldrip, D. M. Follstaedt, P. P. Provencio, D. D. Koleske, and C. R. Abernathy, *Appl. Phys. Lett.* **86**, 241904 (2005).
- <sup>12</sup>W. G. Breiland and K. P. Killeen, *J. Appl. Phys.* **78**, 6726 (1995).
- <sup>13</sup>E. F. Schubert, *Light-Emitting Diodes*, 2nd ed. (Cambridge University Press, Cambridge, 2006), p. 54.